C2.3
Characterization of conductors

Simon A Keys and Damian P Hampshire

C2.3.1 Introduction

There is a large international effort to standardize the test and evaluation methods for industrial superconductors. The Versailles Project on Advanced Materials and Standards (VAMAS) and International Electrotechnical Commission/Technical Committee 90 (IEC/TC90) have worked on producing internationally agreed standards for superconductivity that are required to underpin a mature technology and world-wide industry [1, 2]. The test method authorized by IEC/TC90 for measuring the critical-current (I_C) of industrial Cu/NbTi composite superconductors will soon be published as an international standard [3]. In addition, there is substantial effort directed at standardizing terminology and creating standard test methods for low temperature industrial conductors specifically in the areas of terminology, critical-current, residual resistivity ratio, copper ratio, mechanical properties and surface resistance [3, 4]. Round-robin testing of the high temperature superconductors is also in progress.

Practical conductors are used widely today in many large- and small-scale applications from current leads to magnets. The most important design parameter in such systems is the current carrying capacity of the conductor. For many applications, in order to optimize the use of the conductor, one must know this property as a function of magnetic field, temperature and strain. Most of this paper describes techniques used to test conductors as a function of magnetic field at cryogenic temperatures. It is written so that scientists who are new to critical-current measurements can review the important issues. It considers the so-called strand conductors which include wires and tapes that typically carry currents of up to 600 A. Specialist techniques for characterizing conductors are also highlighted.

This paper has three main sections. The first section includes the basic principles behind making a critical-current measurement and a discussion of the different conventions used to define the current carrying capacity of a conductor. General considerations for mounting and wiring a sample, eliminating-current transfer problems and using relevant measuring equipment are addressed. The methods for analysing the data obtained and the information that can be extracted are outlined in the second section. Finally, a series of case studies are presented which describe good-practice techniques for measuring some of the most important technological materials—NbTi, Nb_3Sn and Ag-sheathed BiSCCO. This paper also refers the reader to specialist techniques that vary considerably from I_C measurements at 4.2 K at the $pV\,m^{-1}$ electric field level to those which determine the form of J_C as a function of magnetic field, temperature and strain.

C2.3.2 General principles for measuring I_C when testing conductors

C2.3.2 Four-terminal critical measurements on strand superconductors

There are many different designs for strand conductors. Schematic diagrams for some of the most common are shown in figure C2.3.1. In addition to the superconducting filaments, other components are illustrated including those required to produce the superconducting material itself (e.g. bronze) or to stabilize the conductor when carrying current (e.g. copper, silver). Some of the most important parameters for describing superconducting strands are listed in table C2.3.1. The construction of the strand is important when characterizing its current carrying capacity (cf section C2.3.3). There are many excellent reviews and texts that discuss conductor design [5].

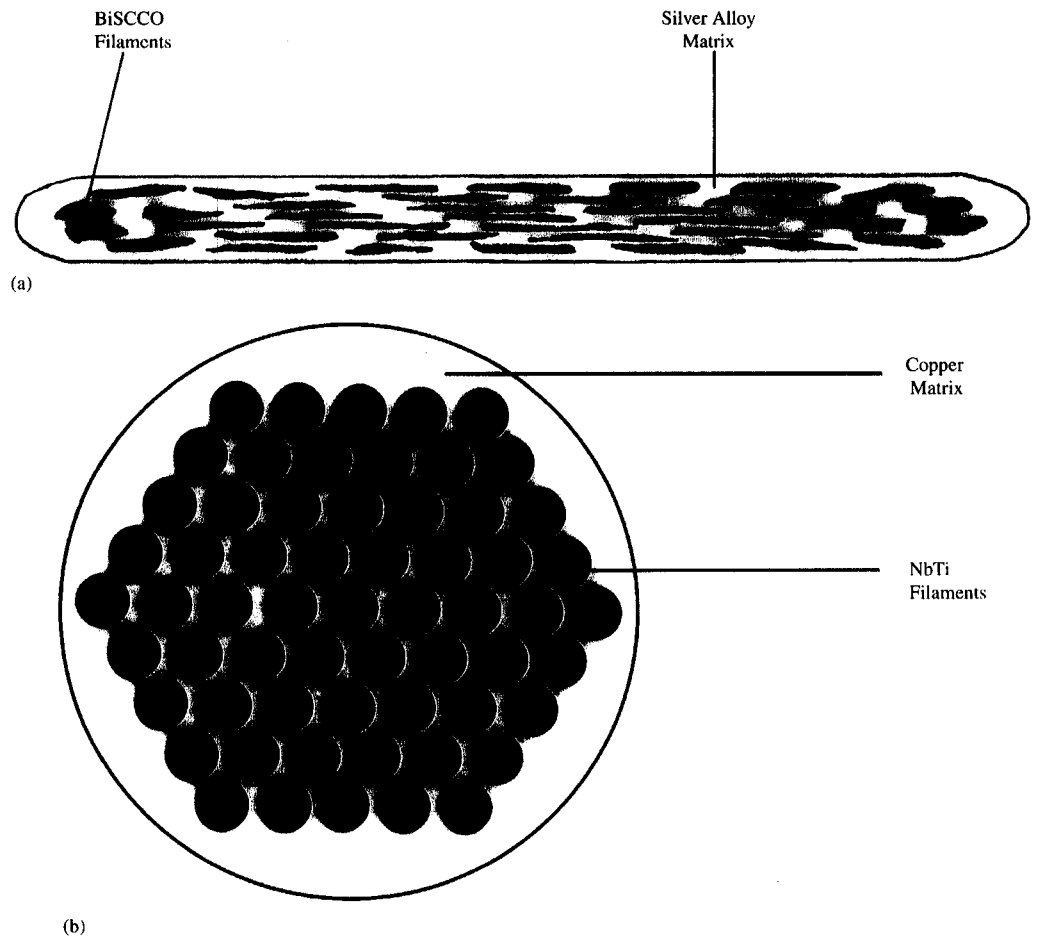

Figure C2.3.1. Schematic diagrams of conductors. (*a*) Ag-sheathed BiSCCO, (*b*) Cu–NbTi, (*c*) modified Jelly Roll Nb_3Sn, and (*d*) multifilamentary bronze route Nb_3Sn.

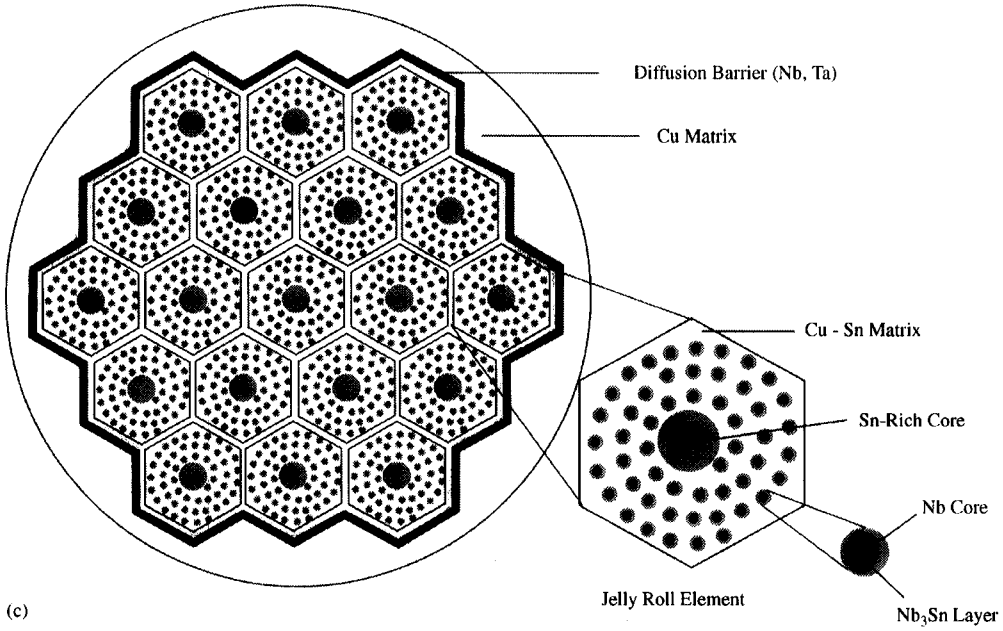

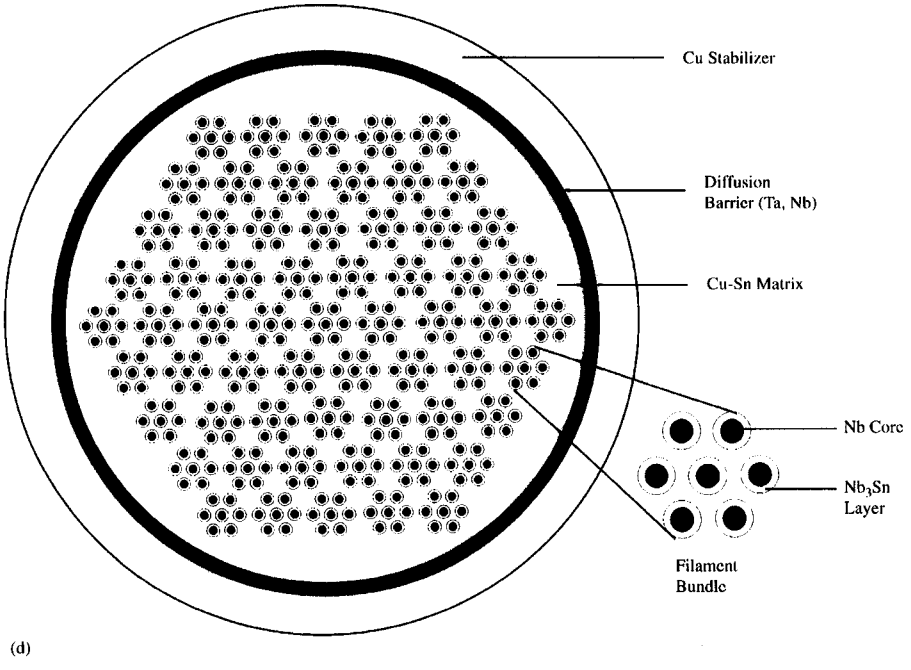

Figure C2.3.1. (Continued)

Table C2.3.1. Typical parameters for a Nb_3Sn strand.

Diameter	1 mm
Number of filaments	6000
Filament diameter	5 μm
Cu/Non Cu ratio	2
RRR of Cu	100
Twist pitch	60 mm
Twist direction	right-hand helix
Critical current at 10 T, 4.2 K	
($10\,\mu V\,m^{-1}$)	150 A
($100\,\mu V\,m^{-1}$)	160 A
n value	45
Hysterisis loss	
(± 5 T transverse field)	$3\,J\,cc^{-1}$
(± 5 T parallel field)	$0.5\,J\,cc^{-1}$

The basic principle behind critical-current measurements is the same as that for four-terminal resistance measurements. The current is applied to the sample by means of current contacts at both ends, and the voltage is measured across a pair of taps positioned across a length of the sample. The current is slowly increased from zero and the voltage across the taps is monitored. Eventually a V–I (or equivalently an E–J) characteristic is measured. This process can be repeated as a function of applied magnetic field as illustrated in figure C2.3.2 (which includes a block diagram of a typical experimental arrangement and typical data). For the data shown, an E-field criteria of either 100 or $10\,\mu V\,m^{-1}$ may be used (cf section C2.3.3) to obtain the critical-current density.

C2.3.2.2 Sample geometry and wiring

There are four different sample geometries that are most commonly used for measuring critical-current, as shown in figure C2.3.3. These are the short straight, long straight, hairpin and coil geometries. The short straight geometry is most often used for conductors that are still in development where homogeneous long lengths of conductors are not available. The coil geometry is commonly used to test long lengths of conductors that are available commercially. The hairpin and coil geometries are used for samples where current transfer from the current leads into the conductor are a problem (cf current transfer section in C2.3.2). In general, the section of the conductor to be measured is perpendicular to the applied magnetic field. This orientation gives the lowest critical-current, and therefore provides the most useful (limiting) case for high field applications [6, 7].

C2.3.2.3 Short straight geometry

The short straight geometry is the simplest configuration. The short sample fits into the bore of a solenoidal magnet as shown in figure C2.3.3(a). No bending of the sample is required during mounting. The sample is easily supported against the Lorentz forces present when performing critical-current measurements in applied magnetic fields, which is particularly important for brittle superconductors. The short sample geometry generates the least self-field of all the configurations. The width of the bore (or cryostat tail) obviously provides a limiting size. Figure C2.3.3(b) shows how the short sample

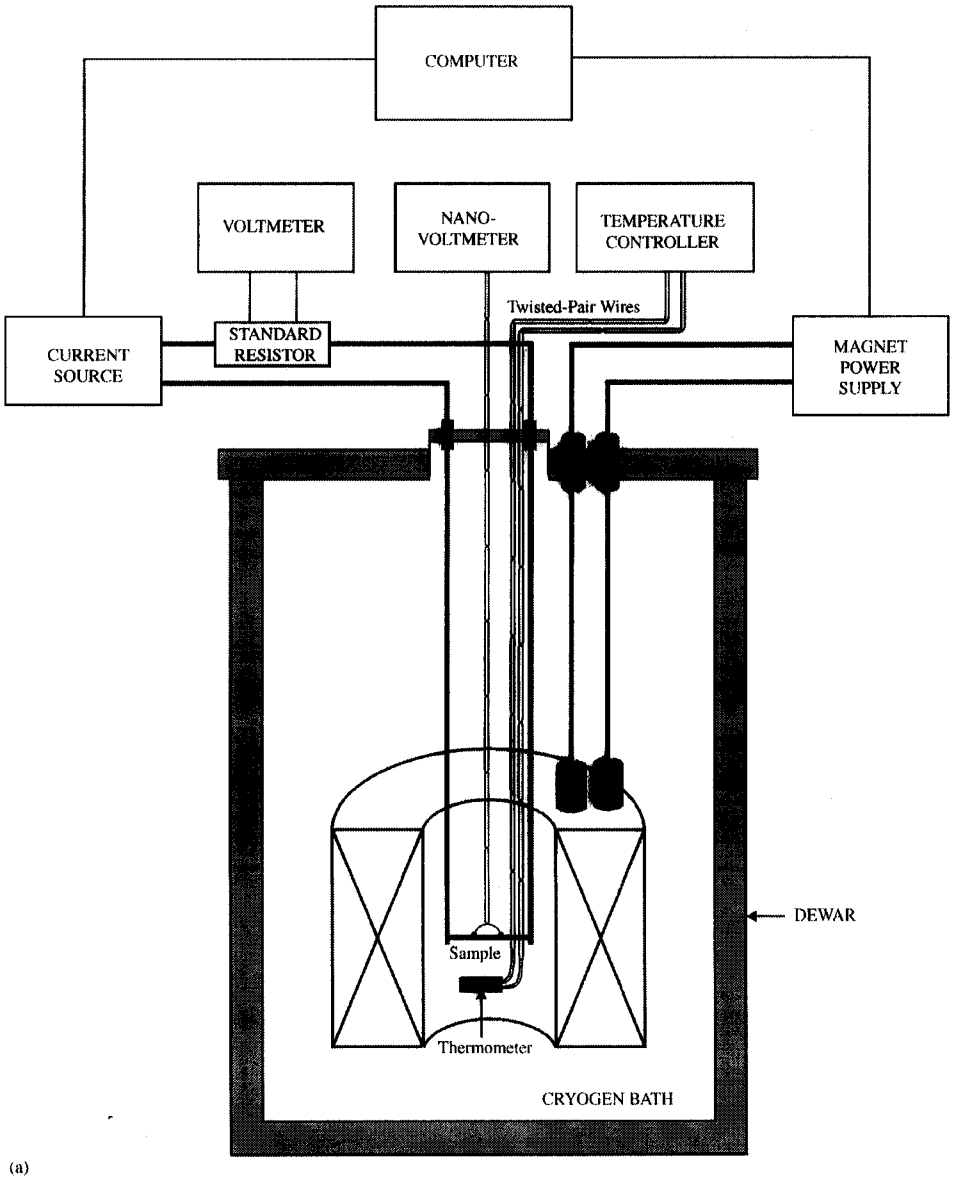

Figure C2.3.2. (*a*) A block diagram of equipment for measuring critical-current density in strand conductors, and (*b*) typical E–J characteristics generated for a Nb_3Al strand [76]. The characteristics were generated as a function of field at 4.2 K. A 21-point smooth has been applied to reduce the noise from the raw data without altering the shape of the transition.

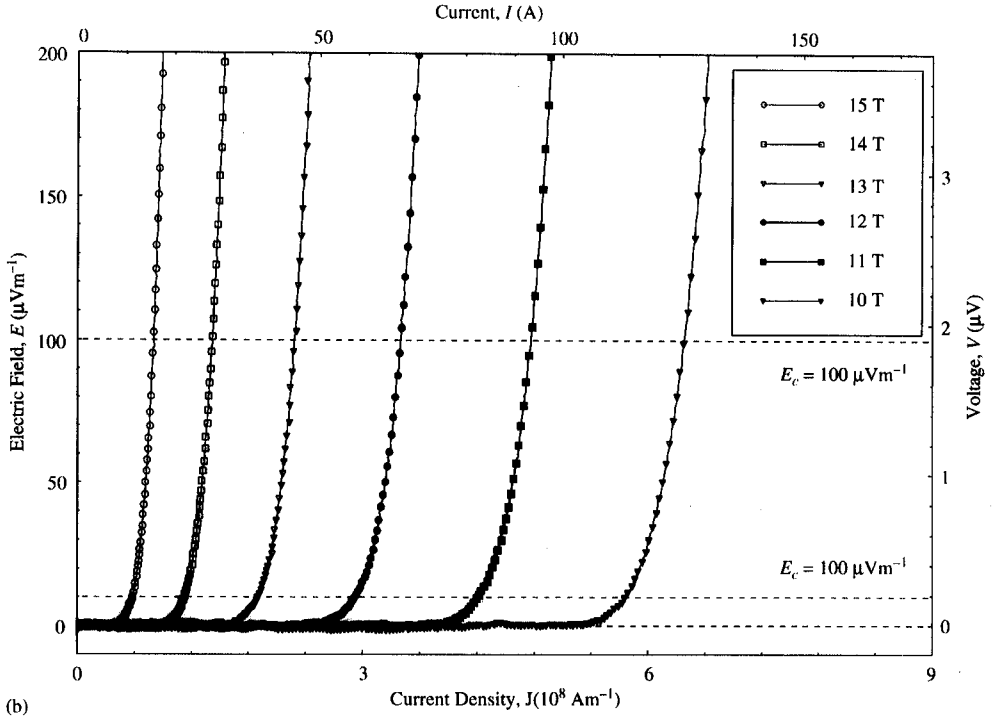

Figure C2.3.2. (Continued)

geometry can be used with a split pair magnet to measure the dependence of critical-current on the orientation of current flow with respect to the direction of the applied field.

The short sample geometry provides the least sensitive E-field criterion for the determination of J_C because of the short measuring length between the voltage taps. The orientation of the sample to the current leads means that there is a relatively small contact area for the current to penetrate into the sample compared with the other configurations. This, in turn, increases the contact resistance and heating. The reduced space around the sample limits the distance over which the current can distribute into the superconducting filaments. If the current has not transferred into the superconducting filaments, the voltage recorded across the taps, or dissipation, is associated with the current that has remained in the normal matrix. Hence, voltage taps need to be sufficiently separated from each other to allow sensitive E-field measurements to be made but also sufficiently separated from the current leads to avoid the problem of current transfer. Current transfer into the superconducting filaments is an important problem for measurements on small samples and will be addressed in more detail below.

C2.3.2.4 Long straight geometry

A much greater length of sample is used in the long straight geometry, as shown in figure C2.3.3(*c*). The voltage taps are in the homogenous region of the magnet and are well separated from the region where the current transfers from the current leads into the superconductor. A greater length of the sample is in contact with the current leads. This larger contact area reduces contact resistance and hence heating in

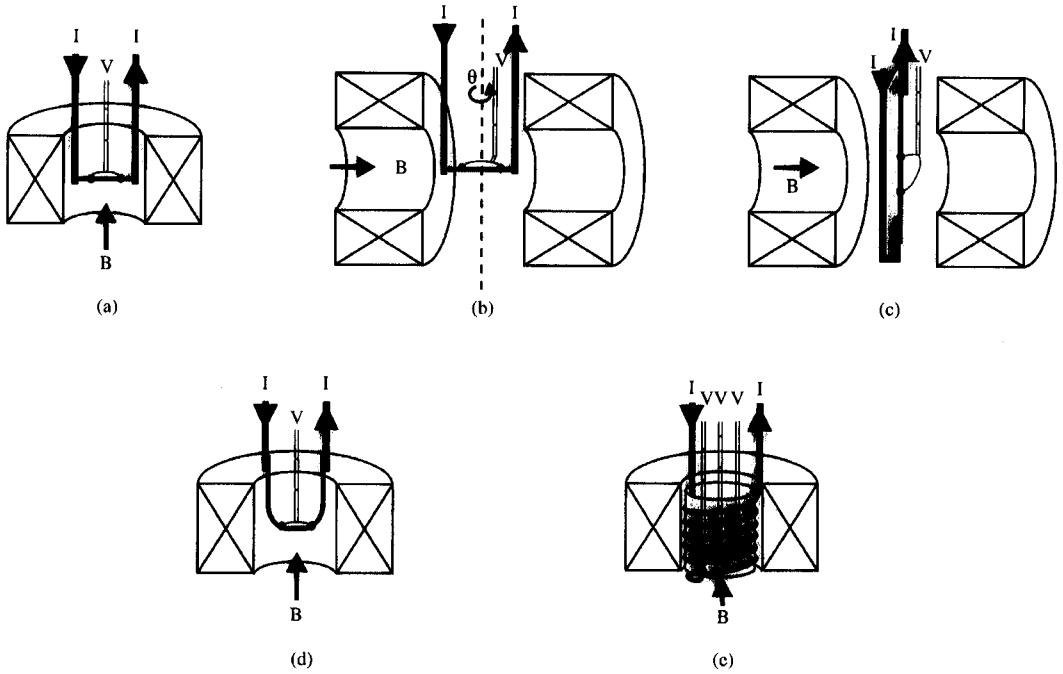

Figure C2.3.3. Different geometries for performing critical-current measurements. (*a*) Short straight as used in solenoidal magnets, (*b*) short straight for finding the angular dependence of critical-current with magnetic field, (*c*) long straight, (*d*) hairpin, and (*e*) coil.

this area. The longer length provides a longer measuring region for the voltage taps, leading to increased *E*-field sensitivity. In this geometry, however, the sample will no longer fit inside the narrow bore of a standard solenoidal magnet so split-pair (or Helmholtz) magnets are used, which are more expensive and do not reach as high fields. The homogeneity of the magnet determines the maximum length over which the voltage taps can be placed.

C2.3.2.5 Hairpin geometry

The hairpin geometry shown in figure C2.3.3(*d*) reduces the contact resistance between the leads and the conductor, and hence reduces current transfer effects in a similar way to the long straight sample geometry. As the current leads are not near the voltage measurements region, a longer measuring distance between the voltage taps can be used, and hence a better *E*-field sensitivity is achieved than in the short straight geometry. The hairpin geometry is suitable for ductile superconductors such as NbTi and conductors that can be reacted into the required shape (e.g. Nb_3Sn). This geometry is not preferred for conductors that cannot be reacted in the hairpin shape, however, due to the strain produced in the sample on forming this configuration. Another aspect of this geometry is the curved nature of the sample. If the orientation of the conductor between the voltage taps varies with respect to the direction of applied magnetic field (e.g., of semi-circular shape) then the measured critical-current will represent an angular average over applied field. A flat-bottomed hairpin is therefore

preferable to a round-bottomed hairpin. Particular care must be taken to avoid damaging the sample when fabricating flat-bottomed samples.

C2.3.2.6 Coil geometry

The coil geometry (figure C2.3.3(*e*)) is most commonly used for testing long lengths of conductor. It is suitable for ductile materials and conductors that can be reacted in the coil shape. The length of conductor used is the largest of all geometries, which means that the voltage taps can be placed the greatest distance apart, leading to the best *E*-field sensitivity. The contact resistance and the current transfer effect can be largely removed for this arrangement. Although the sample is oriented at an angle to the applied magnetic field, all parts of it experience the same offset angle, which generally has little effect. For example, in Nb_3Sn, a 7° pitch represents a change in I_C of only 2% [6]. The coil geometry also provides the opportunity to investigate the homogeneity of the conductor by placing multiple sets of voltage taps along the sample.

C2.3.2.7 Voltage wiring

There are many sources of voltage noise that can affect J_C measurements. It is important to twist the voltage tap wires together and tie them down in order to prevent them from producing inductive voltage noise by moving in the magnetic field because of the flow of cryogenic gas. The area between the voltage wires and the sample should also be minimized to reduce the inductive loop area further. This procedure minimizes inductive voltages which are produced either as the current through the conductor is increased or from the ripple in the applied magnetic field. For straight and hairpin samples, the voltage wires simply run along the surface of the conductor as shown in figure C2.3.3. For the coil geometry, where the distance between voltage taps can be several turns, the wire from the first voltage tap should run alongside the sample until the second voltage tap. From there the wires should be twisted together. Other sources of voltage noise include thermoelectric, offset, ground loop, common mode and current transfer voltages [8]. If these voltages stay constant during the measurement then they can be simply subtracted from the trace. This is achieved by comparing the voltage at zero current before and after the trace is measured. For the most sensitive voltage measurements, the twisted pair of voltage wires should be continuous from the sample to the voltmeter. In this case, the thermoelectric voltages are minimized since there are no joints in the wire.

C2.3.2.8 Current leads

The design of the current leads varies widely, depending on the application. The temperature gradient along sophisticated current leads, for example, can be controlled by more than one cryogenic liquid and/or the operation of cryocooler. In general, current leads must transport sufficiently large current without thermal runaway or burnout, have low electrical resistance so they do not generate much additional heat in the system and have low thermal conductivity to minimize static boil-off.

Unfortunately, a room-temperature superconductor which may have ideal properties for current leads has not yet been discovered. Nevertheless, the high temperature oxide superconductors are being developed to reduce power consumption and operating costs significantly in large-scale systems. Here, some general design principles are considered for current leads that are made exclusively of metals and commonly used in testing strand superconductors. This will provide order of magnitude values for the size of current leads to aid scientists new to these measurements. For some detailed analysis, the reader is referred to two excellent reviews in the literature [5, 9]. In simple terms, the design of the current leads can be separated into three sections. The upper part of the lead, including the external power lead, generally includes a region where there is almost no gas flow. It is important in this region that the lead is

sufficiently large that it does not burn out. In the middle section, there is the temperature difference from room temperature to the temperature of the cryogen. One must ensure that all the available enthalpy from the flowing cryogenic vapour is used to cool the lead in this region. In optimal design configurations, brass is often the preferred material. Tubes are used which are sufficiently bulky to provide a large surface area for efficient vapour cooling and far less likely to burn out than, for example, copper if temporarily operated outside optimal conditions [9]. An optimized constant diameter brass lead operating from room temperature to liquid helium carries a current given by the condition $IL/A \sim 1.5 \times 10^6\,\mathrm{A\,m^{-1}}$ (where I is the maximum current carried by the lead, L is the length of the lead and A is the cross-sectional area (CSA) of the brass). Hence for a 1 m lead, the current density in the brass should be $150\,\mathrm{A\,cm^{-2}}$. Under these conditions, the leads are sufficiently large that the resistive heating is not excessive at operating current, but sufficiently small to minimise static boil-off. The heat load (Q) into the helium cryogen is typically $1.08\,\mathrm{W\,kA^{-1}}$ or 1.4 l of liquid helium per hour per kA. For brass leads vapour cooled with a nitrogen cryogen, $IL/A \sim 8 \times 10^5\,\mathrm{A\,m^{-1}}$ and $Q = 25\,\mathrm{W\,kA^{-1}}$ [9]. The lead in the bottom section of the device, which is submerged in the cryogen, should be relatively bulky to minimize resistive losses and, if possible, incorporate superconducting wires in parallel. The leads should also be large enough to prevent film boiling of the liquid cryogen [5]. During film boiling, the lead is enveloped by a layer of insulating gas which results in a rapid temperature rise of the current lead, and can change the sample temperature.

C2.3.2.9 Material dependant issues

Experimental testing of conductors can involve making nanovolt measurements in high magnetic fields with hundreds of amperes flowing through the conductor. The brittle nature of some conductors and the high Lorentz forces present mean that the conductor must be fastened securely to prevent the sample from moving and subsequently becoming damaged. Even for ductile conductors, sample movement may also lead to additional voltage noise, variations in the measured critical-current, or even thermal runaway below I_C.

For straight and hairpin geometries, the sample is simply mounted onto the planar surface of the sample holder after reaction or fabrication. For the more complicated coil geometry, ductile materials are wound directly onto the cylindrical sample holder for testing. For brittle materials, conductors are either directly reacted on the sample holder or reacted on a mandrel in the furnace and then transferred after reaction onto the sample holder. The direction of the Lorentz force per unit length ($\mathbf{F}_L = \mathbf{I} \times \mathbf{B}$) is orientated so that it presses the sample against the sample holder and facilitates using less bonding agent to hold the sample in position. Bonding agents include G.E. Varnish, stycast, vacuum grease and solder. A high strength bonding material (e.g. epoxy or solder) is required if large Lorentz forces are present, since a low strength material such as grease may not stop the sample from moving. However, covering a sample with excess bonding agent must be avoided since this will inhibit the transfer of heat from the sample to the cryogen and can reduce the maximum measurable critical-current.

It is important to try to match the coefficient of thermal contraction for the sample holder to that of the conductor. This ensures that there is no additional stress applied to the sample which may affect I_C when the conductor is cooled from room temperature (or the soldering temperature if solder is the bonding agent) to the cryogenic testing temperature. The coefficient of thermal contraction is shown in figure C2.3.4, for some important cryogenic materials. Figure C2.3.4(a) shows thermal contraction data for various superconducting compounds, composites and matrix materials [10–15]. It should be noted that the thermal contraction of the composites will depend ultimately on the construction of the wire. The thermal contraction for Nb_3Sn at 4.2 K, for example, can be 0.21% (as shown in figure C2.3.4(a) [13]) although these comprehensive data were taken on a six-stranded cable indium soldered to a central tungsten. In the VAMAS work, contractions of 0.26–0.28% were reported from room temperature to

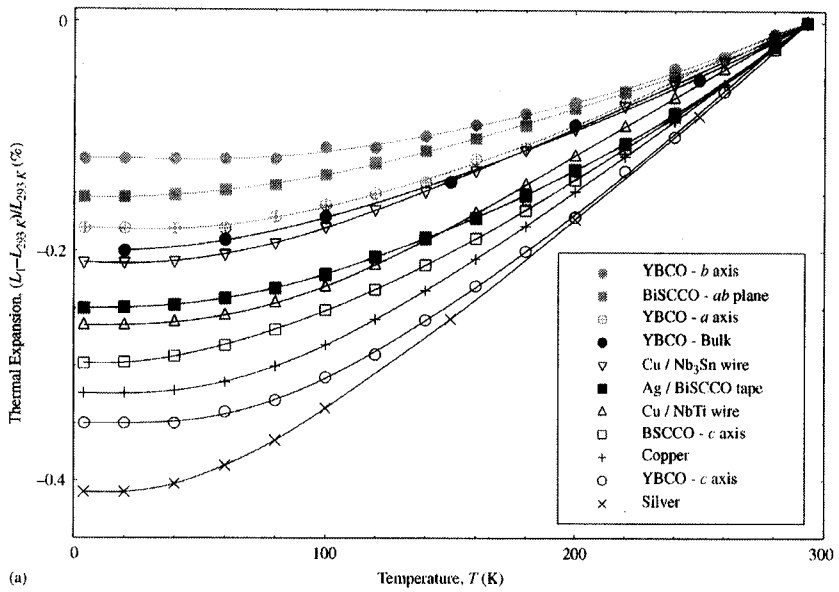

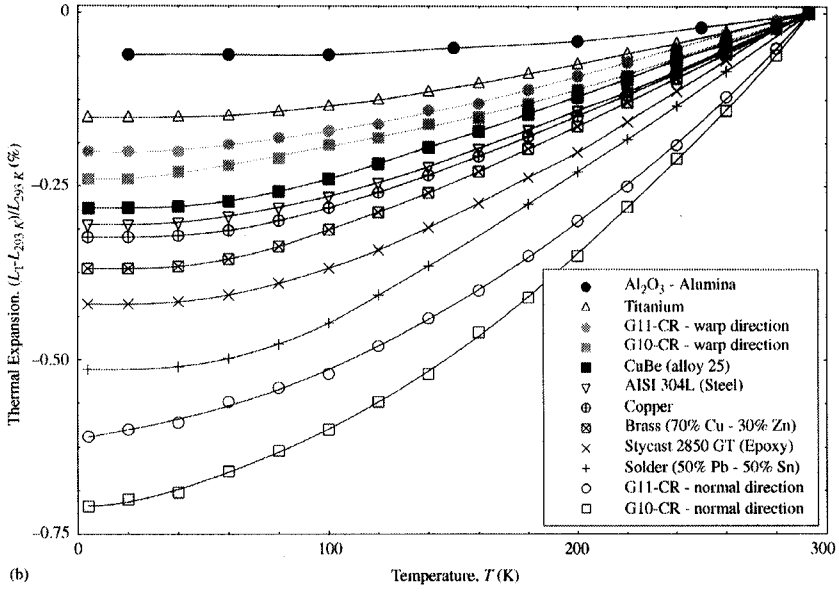

Figure C2.3.4. Thermal expansion as a function of temperature for (*a*) superconducting compounds, composites and matrix materials [10–15]—the Nb_3Sn conductor includes a tungsten core and (*b*) mandrel materials and bonding agents [11, 18–20].

77 K [16, 17]. Figure C2.3.4(*b*) shows the thermal contraction for various common mandrel or bonding materials [11, 18–20]. This parameter for G10-CR and G11-CR is similar in the fill and warp directions. The difference between the thermal contraction of the sample holder and the sample is transmitted between the two by the bonding agent. If a large amount of bonding material is used, both the sample holder and bonding material contribute to the net stress on the sample. The stronger the bonding material, the greater the strain produced by any differential thermal contraction between the sample holder and conductor. The type of bonding agent used must therefore be considered carefully for each particular experiment (see case studies in section C2.3.4).

C2.3.2.10 The current transfer problem

There are two forms of current transfer. The first of these is the initial transfer of current from the current leads into the conductor. Measurements of J_C are most reliable with the voltage taps as far away as possible from the current transfer regions in the vicinity of the current leads. This ensures that the properties of the conductor alone are measured, rather than the properties of the current lead joint resistances. The second current transfer process is between filaments and is generally due to a distribution in I_C. This process depends on the detailed structure and materials in the composite conductor, including the size and distribution of the filaments within the conductor matrix.

In order to transfer current from the current leads into the superconducting filaments, the current must pass through an ohmic matrix or sheath. The voltages produced in the current transfer region increase linearly with current (unless, of course, there is heating in the sample). It has been shown [21] that the minimum distance required to allow for current transfer to a monocore conductor is given by;

$$L = d\sqrt{\frac{0.1}{n}\frac{\rho_m}{\rho^*}} \tag{C2.3.1}$$

where d is the diameter of the filament region of the wire (i.e., the area of the wire containing the superconductor filaments), n is the order of transition which describes the shape of the V–I curve for the superconductor (cf section C2.3.3), ρ_m is the resistivity of the matrix, and ρ^* is the resistivity criterion used to define the critical-current density. This equation yields typical current transfer distances of approximately $30d$ for Nb_3Sn and $3d$ for NbTi [6]. The increased current transfer length for Nb_3Sn compared with NbTi is due to the lower values of n (i.e. 20 for Nb_3Sn compared to 40 for NbTi), and the large resistivity of the matrix (bronze for Nb_3Sn compared to pure copper for NbTi). In BiSCCO 2223 and 2122, the transfer lengths were found to be of order a millimetre at 4.2 K, and tenths of millimetres at 77 K [22]. This unexpected temperature dependence was attributed to a large boundary resistance at the interface between the superconductor and the silver sheath.

The current transfer lengths affect directly the choice of sample geometry. Samples are typically no longer than 25 mm in the short straight geometry. This means that measurements on conductors with high resistivity matrix (e.g. bronze route Nb_3Sn) are best not made using the short sample geometry. However, because the current transfer is not an intrinsic property of the wire, the resistive voltage can be subtracted from the V–I trace [23]. Note that when testing conductors with twisted filaments (which is required in commercial conductors to minimize ac losses), the current contact length should be greater than the twist pitch of the sample to allow the current to enter the filaments evenly [24].

The second type of current transfer is an intrinsic property of the conductor. It is particularly important for ac applications where currents can redistribute between the filaments. In dc applications, a quantitative picture of the dissipative state in inhomogeneous high J_C conductors depends on the E-field range under investigation. At low E-fields, for example in nuclear magnetic resonance (or persistent mode) applications, the superconducting filaments may have a resistance that is still much smaller than

that of the matrix. In this case, the V–I transition is largely unaffected by the matrix and the current transfer is not important. In high E-fields, sausaging of the filaments or inhomogeneities may mean the local I_C in a filament is exceeded, current passes through the matrix either back into the sausaged filament or into another filament [22].

C2.3.2.11 External circuitry

Current source and voltmeter

A smooth current source and nanovoltmeter are typically used under computer control for making J_C measurements. The current through the conductor is usually recorded by measuring the voltage drop across a standard resistor, and the voltage across the conductor by the nanovoltmeter, as shown in figure C2.3.2. The sensitivity and response time of the nanovoltmeter is dependant on the quality of the instrument and the filters used. Voltages at about 100 nV can be measured over an interval of around 50 ms. Standard good practice must be observed when using filters to reduce the voltage noise on a V–I characteristic. In general, the greater the filter used, the larger the time delay before the correct voltage reading is reached. If the response time of the filtering mode is too long, the apparent voltage will be less than the actual voltage, and the V–I transition will artificially broaden giving a false value for I_C. Measurements below the 10 nV range are possible in low noise systems with long measurement times. Noise levels can be improved if unfiltered data are measured by computer, with subsequent editing of outlying points and numerically smoothing the data [25]. The current source itself can be a source of voltage noise. For example, using a analogue nanovoltmeter it has been found that a battery power supply gave a noise level during the measurement of ~2 nV, whereas a silicon controlled rectifier gave ~100 nV [6].

In the most widely used measurement technique, the current is simply ramped at a constant rate until the required voltage is generated across the sample to determine J_C The measurement should be sufficiently slow that the V–I trace does not depend on the rate of increase of current. The rate of increase of current must be small enough that inductive voltages generated vary by less than the voltage used to determine J_C Other factors that limit the ramp rate or the current are possible sample movement and induced eddy currents in metallic sample holders and probe components which cause heating. In the stepped method technique, point-wise data are taken with a delay to allow the inductive voltage to decay. A third method is to ramp quickly to below I_C, wait for the inductive voltage to decay and then sweep the current very slowly through the transition. Pulsed techniques are also used (cf section C2.3.4) and at high E-fields typically agree with dc methods to better than ~0.2% [26] but usually with higher noise levels. A calibrated superconducting simulator is available to assess experimental procedure [27].

Most experimental arrangements also incorporate some form of quench pr otection device. This is particularly important when using unstabalized conductors where there is significant risk of burning out the sample. The protection automatically resets the current to zero when a pre-determined voltage across the sample is reached. Quench protection can be computer controlled or included as an independent analogue component [6].

Magnetic field

The magnetic field for critical-current measurements is often provided by using a superconducting magnet. These systems can produce fields of up to ~23 T for a solenoidal type magnet and about 15 T for a split pair magnet. In the VAMAS Nb_3Sn project, it was recommended that the field for testing conductors should be accurate to 1% and have a precision of 0.5%. The random deviation of magnet field should be less than 0.5% and its homogeneity should be of uniformity ± 1% over the length of the sample between the voltage taps [28].

Above ~1 T, high field superconducting magnets exhibit an almost linear dependence between the field generated and the current through the magnet. At low fields, however, hysteresis can cause problems when trying to determine the low field properties of conductors. There are various approaches that can be taken to eliminate errors due to the remnant field. The field at the sample can be measured independently using a Hall or nuclear magnetic resonance probe. This is the only technique that allows the hysteretic behaviour of J_C for the conductor to be measured in increasing and decreasing applied field. The remnant field can be reduced to typically less than ± 20 mT by degaussing the magnet. This involves sweeping the field from a high value through zero and back, reducing the amplitude and sweep rate at each reversal. An alternative is to initiate a controlled quench in the magnet. This can be done by means of a carefully designed quench heater [29] incorporated within the turns of the magnet which forces the temperature of the superconducting windings to above T_C. This completely destroys the remnant field. However, the dangers of damaging the magnet by quenching should be noted.

For dc fields of up to ~30 T, high power resistive magnets (generally available at international facilities) can also be used. These magnets produce no remnant field. However, the water cooling and power required for this design of magnet are large with commensurate mechanical vibrations in the magnet system, which can cause additional sources of voltage noise.

C2.3.3 Voltage–current characteristics and critical-current analysis

C2.3.3.1 Defining the critical-current (I_C) and the critical density (J_C)

A generic voltage–current (V–I) characteristic is shown in figure C2.3.5 with the various conventions used to define the critical-current. The choice of convention depends on how the data are to be used. For example, in standard high field solenoids the engineering current density at an electric field criterion of about 10 $\mu V\,m^{-1}$ will determine the performance of the magnet. For Nuclear Magnetic Resonance applications, on the other hand, where the magnet is in persistent mode, the current density at an E-field about six orders of magnitude lower is required. The critical-current can consequently be strongly dependent on the chosen criterion [6].

The most commonly used convention for defining critical-current (I_C) is an electric field criterion (E_C) given by $E_C = V/L$, where V is the voltage difference between the voltage taps and L is the length of wire between the voltage taps. Typically the electric field used to define I_C is 10 or 100 $\mu V\,m^{-1}$. I_C never falls to zero, using such criteria. A resistive (ohmic) sample which has no curvature on the V–I trace will still cross the electric field criteria at some point, leading to a value of I_C. For typical conductors (~1 mm diameter), this non-superconducting current (for example, in the Cu that stabilizes the conductor) ranges from 10–500 mA when the E-field is 10 $\mu V\,m^{-1}$, which is not significant in engineering applications (although as discussed below it can be important for more fundamental studies). In the case of short straight geometry where the measurement distance is typically no longer than 1 cm, a voltage sensitivity of less than 100 nV is required to obtain an electric field criteria of 10 $\mu V\,m^{-1}$. It should be noted, however, that low current densities obtained using this criterion can be characteristic of non-superconducting metals.

The resistivity criterion (ρ_c) for J_C is given by $\rho_c = VA/IL$, where V is the voltage difference between the voltage taps, L is the length of the wire between the voltage taps, A is the CSA of the wire and I is the current through the wire. Values of J_C are often quoted at ρ_c of 10^{-14} or 10^{-13} Ωm. The critical-current using the resistivity criteria disappears at high fields as long as that chosen is less than the normal state resistivity of the conductor. However, problems can arise in fundamental studies if the resistivity criterion is used. For example, some superconductors do not show a zero-resistance region in high fields. If the (superconducting) flux-flow region has a resistivity above that of the resistivity criterion, I_C is zero but the conductor remains in the superconducting state.

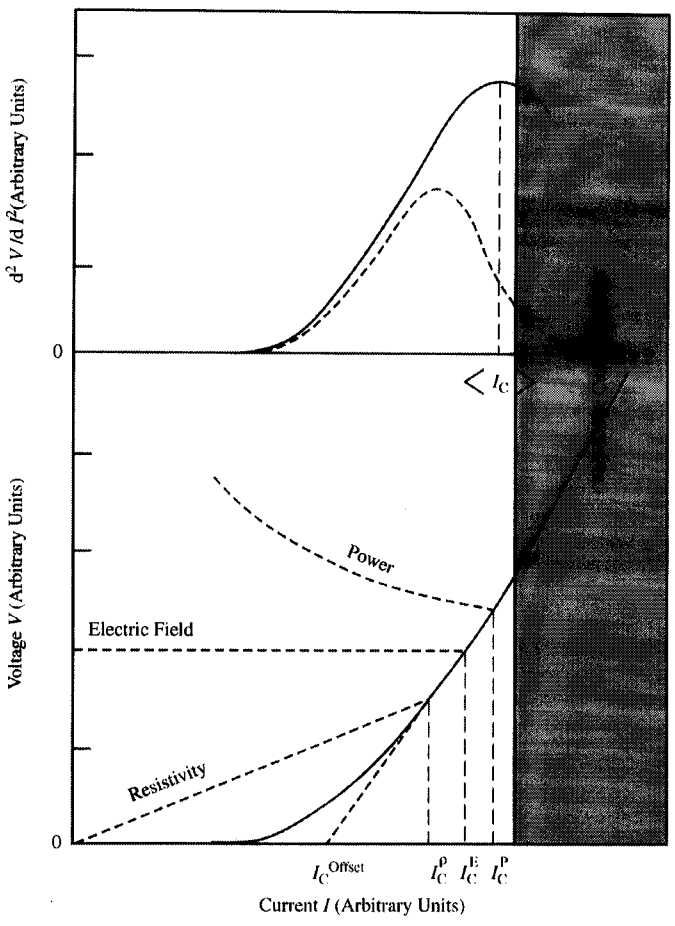

Figure C2.3.5. The lower panel shows the conventions used to define I_C—the electric field, resistivity and power criteria as well as the offset method. The upper panel shows d^2V/dI^2. The dotted line is for the conductor and shunt [32]. The solid line is for the superconductor alone and can be equated to the distribution in I_C.

A power criterion (P_C) defined by $P_C = IV$, is sometimes used in large-scale applications. It can be a useful criterion in magnet design to specify the maximum allowed consumption of cryogen and thus a suitable working current.

The offset method [23] is a method for calculating I_C which attempts to minimize the problems associated with the electrical field or resistivity criterion. I_C is calculated in two stages. A tangent to the V–I curve is constructed at an electric field criteria given by E_C. The critical-current is then defined as the current at which the tangent is extrapolated to zero voltage. This procedure provides an attempt to subtract the current flowing in the non-superconducting components from the total current which can be useful for samples where there is a large shunt in parallel with the superconductor.

The critical-current density can be calculated in three ways once the critical-current has been measured. For engineering applications, the conductor is treated as a single entity. The V–I

characteristic for the entire conductor including the stabilizing material and the matrix is required. The engineering critical-current density (J_C^e or J_e) is defined as the critical-current divided by the CSA of the entire conductor. This is the important parameter when designing systems such as magnets. The second definition of current density is relevant for comparing and developing conductors of different superconducting materials. It can be seen in figure C2.3.1 that, in contrast to NbTi and BiSCCO, Nb_3Sn conductor has matrix material such as (tin depleted) bronze, which is neither superconducting nor contributes to stabilizing the conductor. However, it is required in the processing of the conductor and cannot be removed. Hence $J_{C(Non\text{-}Cu)}$ can be calculated using the area of the superconductor that is not matrix material (i.e. non-Cu or non-Ag). This provides the second definition of J_C and is particularly useful for wire manufacturers. In fundamental studies, the critical-current density in the superconducting layer alone is required. Measuring the CSA in NbTi or BiSCCO is relatively straightforward. However, if there are fine superconducting filaments as in Nb_3Sn or Nb_3Al conductors, it can require electron microscopy to determine the CSA of all the superconducting layers alone.

C2.3.3.2 Flux creep, flux flow and damage

In this section, the difficulties that can occur in interpreting V–I traces are discussed. Poor experimental technique can produce artefacts in the data which can be very misleading, particularly when measuring brittle superconductors. Figure C2.3.6 shows five V–I characteristics that will be discussed in this context. These data are schematic representations of actual characteristics with their important features enhanced, and can be explained as follows:

Figure 2.3.6(*a*) There is a resistive (current transfer) region at low currents due to an insufficient separation between the current leads and the voltage taps. The transition to the normal conducting state is evident at high currents.

Figure 2.3.6(*b*) Flux creep is evident at low currents. At high currents, the transition rises sharply as flux flow sets in.

Figure 2.3.6(*c*) Zero resistance occurs at low currents with supercurrent flowing in undamaged filaments. At intermediate currents, there is a resistance due to current transfer in and out of a limited number of damaged filaments. At high currents, the conductor is in the flux-flow state.

Figure 2.3.6(*d*) There is a zero-resistance region followed by a flux-flow transition.

Figure 2.3.6(*e*) There is zero-resistance until a quench occurs in the conductor. This is followed by heating and thermal runaway.

The explanations provided for the curves (*a*)–(*e*) are clearly not unique. If the effects of heating due to filament damage or tunnelling across cracks are introduced for example, one can relatively easily provide a different explanation for any of the V–I traces. The critical point to note from these data is that one can misinterpret curves (*a*), (*c*) and (*e*), which do not show the intrinsic properties of the conductor, for curves (*b*) and (*d*) which are intrinsic. From the V–I trace alone, it may not be possible to distinguish reliably between flux creep (intrinsic to the conductor) and current transfer (and heating), which can occur because of damage or poor measuring technique. It is concluded that it is *essential* to employ good practice in mounting samples and is preferable that more than one length of the conductor is measured to ensure the reliability of the results.

C2.3.3.3 Shape of the transition

The shape of the V–I characteristic of a conductor can be described using

$$E = \alpha J^n \tag{C2.3.2}$$

or less frequently

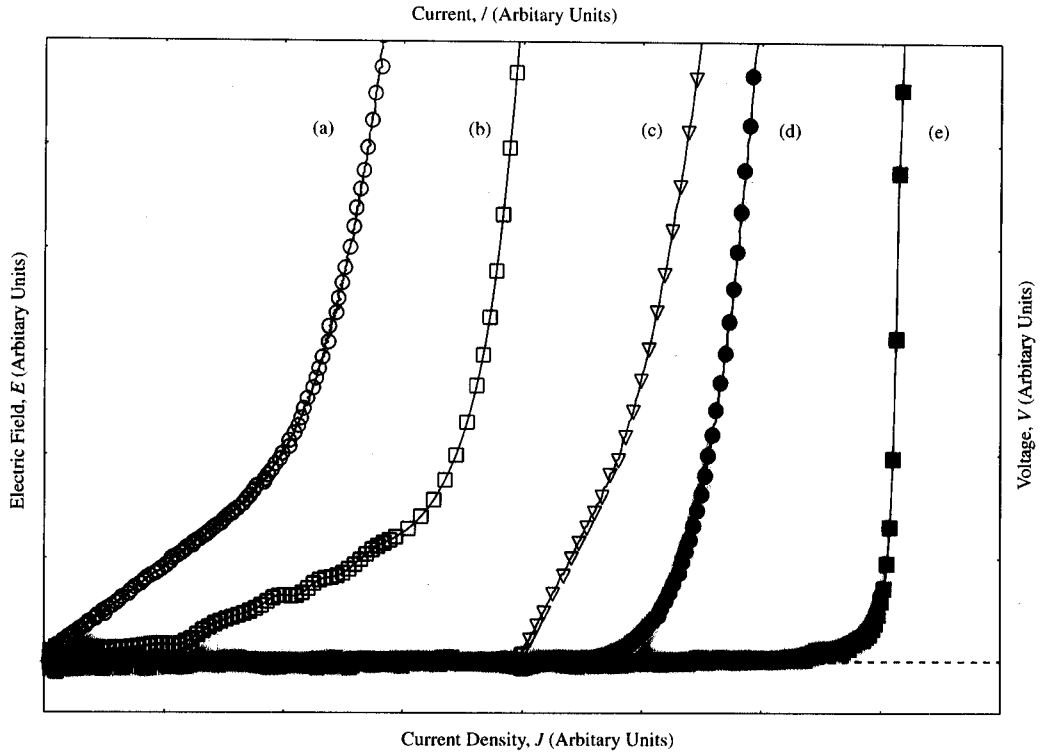

Figure C2.3.6. Schematic V–I characteristics illustrating flux creep, flux flow, thermal runaway and current transfer.

$$E = E_0 \exp\left(\frac{J - J_0}{J_E}\right) \tag{C2.3.3}$$

where α, E_0, n, J_0 and J_E are all experimental or materials constants. The n-value is often called the order of transition or index. It is important to note that the n characterizes the entire conducting path between the voltage taps, including the stabilizing material. If the conductor is mounted on a metallic (low resistance) sample holder, although current sharing through the shunt may only affect I_C slightly (depending on the criterion used), the value of n can decrease significantly [30]. High n values tend to signify more homogeneous superconductors. Typical values for n lie between 10 and 100 and in engineering applications tend to be used as a figure of merit.

In flux pinning and flux motion studies of conductors, analytic techniques are used to develop the data beyond the empirical expressions for the E–J characteristics and the (arbitrary) conventions used to define J_C. For conductors at low temperature, where thermal activation is not important, the E–J transition of a superconductor can be described by [31].

$$E(J) = \rho \int_0^J (J - J_i) f(J_i) \mathrm{d}J_i \tag{C2.3.4}$$

where J_i is the local critical-current, $f(J_i)$ is the distribution of critical-currents in the sample, and ρ is the resistivity describing flux flow in regions of the superconductor where the current exceeds the local critical-current. In the analysis, the current density terms represent the current density flowing in the superconductor in which case current flowing in the shunt and the stabilizing material of the conductor must be subtracted to obtain the correct $f(J_i)$ function [32]. This has been done by measuring the V–I characteristic above $B_{C2}(T)$ [33].For high temperature superconductors (HTS), this can be achieved by etching off the matrix [32, 34]. By invoking the central limit theorem, it can be assumed that $f(J_i)$ can be described by a normal distribution of the form:

$$f(J_i) = \frac{1}{(2\pi)^{1/2}} \frac{\beta}{J_C} \exp\left\{-\frac{1}{2}\left[\beta\left(\frac{J_i - \bar{J}_C}{J_C}\right)\right]^2\right\}, \quad \beta = \frac{\bar{J}_C}{\sigma(\bar{J}_C)} \tag{C2.3.5}$$

where $\bar{J}_C$ is the average J_C of the distribution and $\sigma(\bar{J}_C)$ is the standard deviation of the critical-current distribution [31, 33]. Good agreement is found between experimental data and equations (C.2.3.4) and (C.2.3.5). Detailed variable temperature, variable field measurements have been completed on NbTi [33, 35], Nb_3Sn [36] and V_3Ga [37] conductors and scaling laws found for ρ, β, n and $\bar{J}_C$. Equating the empirical equation (equation (C.2.3.2)) to the more physical one (equation (C.2.3.4)) at $J = J_C$ [35] gives:

$$\beta = n\left(\frac{2}{\pi}\right)^{1/2} \tag{C2.3.6}$$

This equation is consistent with the empirical finding that homogeneous materials have high values of n (it is not valid for very low n values ($n < 5$) at low E-fields [38, 39]). The distribution of critical-current densities can be derived explicitly making no assumption about the form of the distribution using [38, 40]:

$$f(J_0) = \frac{1}{\rho}\left(\frac{d^2E}{dJ^2}\right)_{J=J_0} \tag{C2.3.7}$$

A graphical representation of this analysis is shown in figure C2.3.5. However, the distribution obtained is sensitive to noise and the algorithm used to calculate the second derivative [41]. It is difficult to measure the distribution at high current because of heating and the local hot spots that occur at high E-field values. This is particularly problematic if the stabilizing material is etched out of the conductor [32].

The formulism used to describe the vortex glass–vortex liquid phase transition in weak-pinning high-T_C superconductors has also been developed to describe the E–J characteristics. Generalized scaling laws have been developed [42] by considering thermal activation and flux pinning. It is clear that similar scaling laws are also to be expected if a distribution in T_C and $B_{C2}(T)$ is introduced. Scaling in the E–J characteristics has been observed in both low temperature [43] and high temperature superconductors [42].

The two approaches for the analysis of E–J characteristics are essentially complementary. At low fields and temperatures, J_C is high and thermal activation may play little role. Sausaging in the conductor filaments, variations in microstructure and composition are important and in these cases one can expect the resultant distribution in J_C to be described using equation (C.2.3.4). At the highest fields and temperatures, the distribution in fundamental properties, thermal activation, percolation and regions of very low J_C may dominate the properties of the conductor. In this case, the phase transition formulism is probably most appropriate. These two formulisms are both being developed to understand better and optimize the distribution and magnitude of J_C in conductors.

C2.3.4 Case studies for testing different materials

C2.3.4.1 I_C as function of field in liquid

This section describes mounting techniques for NbTi, Nb_3Sn and BiSCCO conductors. All of these materials either have been or are currently part of international comparative studies for the standardization of measurement techniques. The typical errors found when measuring each material are also discussed. Very accurate and stable temperature control can be achieved when making critical-current measurements by direct immersion of the conductor in liquid cryogen. However, there are some general points to be aware of when measuring any of these materials:

The vapour pressure of the gas can be monitored to give the temperature of the bath as suggested by the VAMAS Technical Working Party in their standard method for I_C determination of Nb_3Sn wires [28]. Bath temperatures can be determined from standard tables [44]. Temperature errors can occur when using liquid nitrogen if air (primarily oxygen) has dissolved in the nitrogen due to associated changes in the vapour pressure–temperature relation. If atmospheric pressure is used, care must be taken that there is not a build-up of pressure in the dewar as the critical-current transition is reached.

It is prudent to monitor the temperature of the sample during the V–I measurement to ensure there is no heating. The type of thermometer used should be chosen based on its properties in high magnetic field, its sensitivity and its response time.

For measurements in the coil geometry, both metal (normally stainless steel) and glass fibre reinforced plastics/epoxy (FRP) are commonly used for the sample holder. The wire should be wound on to a spirally grooved sample holder to help prevent it from moving during the measurement. The spiral groove should be at an angle no more than 7° to reduce the effects of placing the sample at an angle to the applied magnetic field. Copper ends are fitted to the sample holder and act as current contacts to which the ends of the sample are soldered. The direction of the Lorentz force during measurements should be into the sample holder. The FRP sample holders should be machined from plate stock, so the axis of the tube/cylinder is along the normal direction of the FRP plate. It is less preferred to use rolled FRP tubes with the axis of the tube in 'fill' direction because the thermal contraction is more anisotropic than with machined plate and depends on the dimensions on the tube [45]. The groove should be of 60° V-cross-section with a depth approximately equal to the diameter of the wire. Thin-walled stainless steel sample holders should also be grooved to guide the wire [28]. An important consideration when using metallic sample holders is the current sharing that occurs in the dissipative state. Current sharing can produce a large reduction in the n value particularly if a solder bond is used [30]. For standard testing of commercial wires for engineering purposes, current sharing is best avoided. However, although the technologically important J_c may not be accurately measurable on soldered metallic sample holders, in fundamental studies that require J_C (i.e., for the superconductor alone) even the current sharing through the stabilizing matrix within the conductor should be subtracted from the measured data. In such experiments, one can use soldered metallic sample holders and treat current sharing through the normal shunt and stabilizing material as a single path in parallel with the superconductor. Indeed in such studies, it has been found useful to electroplate a very thin copper layer onto the stainless steel sample holder to ease the soldering process, prevent unstabilized conductors from burning out and ensure that localized damaged sections of the wire do not quench the entire conductor during testing.

When using solder, in particular for attaching voltage taps, it is important not to thermally shock the conductor. For brittle superconductors, a hot-air gun may be used to warm the conductor uniformly to just below the melting point of the solder before using the soldering iron to attach leads. The temperature of the gun can be set using a thermocouple-based thermometer. Low temperature solder such as $In_{0.52}Sn_{0.48}$ (M.P. ~118 °C) can be used to minimize thermal shock [46]. It should also be noted that standard PbSn solder (M.P. ~190 °C) is superconducting at 4.2 K up to ~0.1 T.

In low fields, I_C can be strongly dependent on whether the applied field has been increased or decreased to obtain the required value (i.e. I_C is history dependent) [47–49].

In general, one tries to match the thermal contraction of the sample holder to that of the conductor. The properties of any conductor are determined by all its component parts. The sample holders suggested by the standards testing community have been chosen as appropriate for a reasonable range of the common commercial conductors.

2.3.4.2 NbTi

NbTi is usually measured using the coil geometry. Insulation can be removed chemically using a mixture of phenol/methylene chloride to prevent mechanical damage during sample preparation. Although NbTi is a ductile superconductor and J_C is reasonably insensitive to strain [50], care must be taken to avoid placing any extra strain on the wire during winding.

Both FRP and stainless steel holders can be used. The FRP used is G-11CR (US notation) or EP GC 203 (European notation) which has a thermal contraction similar to NbTi. If the sample is held in place using varnish, a strong epoxy (such as stycast), vacuum grease, or no bond at all, this has little effect on I_C [51]. In the IEC/TC90 standardization of the NbTi critical-current measurement test method, stainless steel sample holders and FRP were used with low temperature adhesives. The use of solder was not recommended. The critical-current values for the samples on steel sample holders were only slightly different to samples mounted on G10 [52].

One of the 'standard measurements' laboratories in the USA (NBS/NIST) has produced a standard reference NbTi material (SRM 1457) that has been tested for long length homogeneity and measured extensively in interlaboratory comparisons. Critical-currents were measured at 2, 4, 6 and 8 T on FRP for temperatures from 3.90 to 4.24 K using electric field criteria from 5 to 20 $\mu V m^{-1}$. The total uncertainty of the reported critical-current values at any of the four magnetic fields was no greater than 2.6% [50]. In a second series of measurements, the uncertainties for the critical-currents (measured at an electric field criteria of 10 $\mu V m^{-1}$) were found to be 1.71 and 1.97%, and the difference between the interlaboratory averages and certified critical-current were 0.2 and 0.3% for 6 and 8 T, respectively [53]. In the IEC/TC90 experiments, the coefficient of variation for samples mounted on FRP (standard deviation divided by the average value) was lower than 2% for I_C measurements from 1 to 7 T [52].

C2.3.4.3 Nb_3Sn

The increased sensitivity of Nb_3Sn to mechanical strain means that care must be taken when mounting samples to avoid degrading J_C prior to measurement. The coil geometry is generally used. Nb_3Sn conductors should be reacted on a stainless steel reaction mandrel of a geometry that closely matches the sample holder. The surface of the reaction mandrel should be heavily oxidized to prevent any diffusion bonding between it and the conductor −800 °C for 3 h in air is usually sufficient. The wire should then be wound on the mandrel for the heat treatment during which brittle Nb_3Sn A15 compound is formed. The sample should then be carefully transferred on to the sample holder taking care not to unduly strain the wire during this operation.

A G10-CR (US notation) (EP GC 201: European notation) or stainless steel measurement mandrel is often used. G-10CR (machined from plate) is similar to G-11CR (used for NbTi), but has a differential thermal contraction better matched to Nb_3Sn [16]. Other materials with similar thermal expansion properties to Nb_3Sn conductors are non-magnetic stainless steels, copper or non-magnetic copper alloys (see figure C2.3.4). As part of the VAMAS report, similar I_C's as a function of magnetic field were found using G10 and stainless steel sample holders. Stainless steel has the advantage that it can be used for both the reaction and measurement, which eliminates the need to transfer the sample. Vacuum grease

was suggested as the bonding agent in the VAMAS test as it is easy to remove from the sample after use. Stycast (a high strength epoxy) was also tested and gave similar I_C's for stainless steel and G-10CR sample holders [54]. The IEC/TC90 round-robin test on Nb_3Sn composite conductors advised explicitly against using a solder bond on the stainless steel. Alumina ceramic can also be used as a dual-purpose mandrel/sample holder, either by itself or as a coating on stainless steel [51]. There is less chance of bonding between the holder and the conductor, but the thermal expansion is not very well matched.

In the VAMAS work on Nb_3Sn, the variation in I_C was obtained from two intercomparisons. The first allowed each laboratory to use their own methods of measuring I_C, the second used the standard method using G10 and vacuum grease described above. The ratio of standard deviation to average value for the first intercomparison was 8.0% for I_C defined at 10 $\mu V\,m^{-1}$ measured at 12 T and 4.2 K. This fell to 2.2% for the second intercomparison using agreed mounting procedures [53].

C2.3.4.4 BiSCCO

It is often not possible to wind high temperature superconducting tapes into coil form due to their brittle nature. Thus, the most common measurements for high T_C tapes use the short straight geometry. The results of the interlaboratory comparisons have been reported, some of which are included below [46].

Both G-10 and brass have been used as sample holders. However, it was reported that the sample was more likely to separate from the substrate when mounted on brass (due to differential thermal contraction) which can damage the samples. Hence, the samples are best bonded to a G10 sample holder using a glass-filled epoxy. Current contacts and voltage taps can be soldered directly to the sample using a low temperature solder. However, some damage inevitably occurs by soldering although successful measurements on short samples can be made by soldering the current leads and using silver paint/epoxy for voltage taps [55]. Methods used for mounting HTS conductors have been discussed [46]. Many BiSCCO conductors are not fully dense. For the Ag-sheathed BiSCCO tape it was observed that the thermal expansion was dependent on thermal cycling, which was attributed to yielding due to an internal stress between the Ag-sheath and the BiSCCO(2223) filaments [15]. Cryogenic liquid can seep into the conductor during measurement. Under these circumstances, it is essential to warm the sample slowly after measurement so the cryogen can escape without blistering the silver matrix [46].

In round-robin testing, the coefficient of variation for a BiSCCO sample premounted by a central laboratory (NIST) were 4.4 (77 K) and 3.2% (4.2 K) [46]. The IEC/TC90 is in the process of developing a dc critical-current test method for Ag-sheathed BiSCCO conductors [56].

C2.3.4.5 Specialist techniques

Pulsed methods for I_C measurements

The most common pulsed method involves increasing the current from zero to a predetermined level in 1–10 ms, measuring the voltage drop along the conductor and ramping back to zero again. The voltage is also measured before and after the pulse to allow for the subtraction of any offset. A series of pulsed measurements can be used to construct the superconducting V–I characteristic [57]. Highly sensitive instruments with rapid response times are required for these measurements. An important advantage of the pulsed method is that if the current contacts are poor (highly resistive), they have limited effect on the measurement because there is no sufficient time during the pulse for the heat to diffuse to the part of the conductor between the voltage taps. Measurements have also been performed using pulsed magnetic fields [58]. In this case, a constant current is applied to the sample, and the voltage generated is recorded. This method has the advantage of allowing measurements to be taken up to the highest fields (> 50 T). The rapid change in magnetic filed, however, causes Eddy current heating which prevents accurate measurement of some samples.

Persistent mode experiments

The V–I characteristics can be found by measuring the decay of the current in a persistent mode coil [59]. A current is induced into a superconducting coil, and the decay of the self-field measured a function of time. The decay can be converted into an equivalent resistance for the conductor. This is presently the only method which gives measurements on long lengths of conductor down to an electric field of a few $pV\,m^{-1}$ relevant for NMR applications. Results obtained on NbTi and Nb_3Sn are in broad agreement with a normal distribution of critical-currents described using equations (C.2.3.4) and (C.2.3.5).

$J_C(B,T)$ – techniques

The variation of critical-current as a function of temperature is critical in assessing conductors for cryogen-free applications and for many large-scale systems for which forced flow helium is used. Over limited temperature ranges, vapour pressure thermometry is best used. With liquid helium, it is possible to vary the temperature between ~1.8 and 5.22 K and with nitrogen from about 55 to about 85 K. The temperature of the liquid is varied by pumping or pressuring.

Techniques have also been developed to measure conductors in an isothermal environment so the temperature can be varied continuously over any temperature range above 1.8 K [60, 61]. Typically, the sample is in intimate contact with a copper thermal block that incorporates a heater and thermometry. A temperature controller maintains the temperature constant as the V–I characteristics are measured. Purpose built and commercial variable temperature cryostats can also provide the required isothermal environment. Both dc continuous and pulsed methods are used to obtain the V–I characteristics [62, 63].

$J_C(B,T,\epsilon)$ – techniques

Due to the brittle nature of most superconducting wires or tapes, the effect of applied strain on critical-current is of great interest, especially for high-field applications where the wires are subject to large Lorentz forces.

Most variable strain data on conductors have been obtained at 4.2 K. The short straight geometry [64, 65] was developed for measuring the effect of tensile uniaxial strain, although the same principles can be applied to long straight samples in split pair magnets in order to overcome the problems of current transfer [66]. The sample is soldered between two copper blocks which act to apply the strain and serve as current contacts. Detailed measurements have been reported on a wide range of conductors in cryogens including Nb_3Sn [64], Nb_3Al [67], $PbMo_6S_8$ [68] and BiSCCO [69–71].

In order to apply compressive uniaxial strain the sample needs to be supported. Two different types of bending springs have been used for this purpose. A U-shaped bending spring (made from brass or steel) has been used [72] to which a flat-bottomed type hairpin sample can be soldered. Compression or extension is applied to the spring by means of a force applied to its legs which either separates them or brings them together. Strain is measured by a strain gauge either mounted directly on the sample, or in close proximity on the spring. Alternatively a helical bending spring can be used which accepts coil type samples [73]. One end of the spring has a torque applied to it whilst the other is held fixed. This mechanism can apply either tension or compression to the sample. Recently this approach has been developed for making variable temperature measurements by placing the spring in an isothermal environment [74, 75]. Typical data are shown in figure C2.3.7 [76].

The effect of transverse stress on critical-current has also been measured [65, 72, 77, 78]. The samples were placed between a fixed position pressure block and a movable pressure block. The stress is applied by compressing the sample. Although it is not possible to measure the strain in this configuration, it is possible to obtain equivalent stresses for uniaxial strains to allow direct comparison between measurements. The V–I characteristics are measured at a series of different stresses. It has been

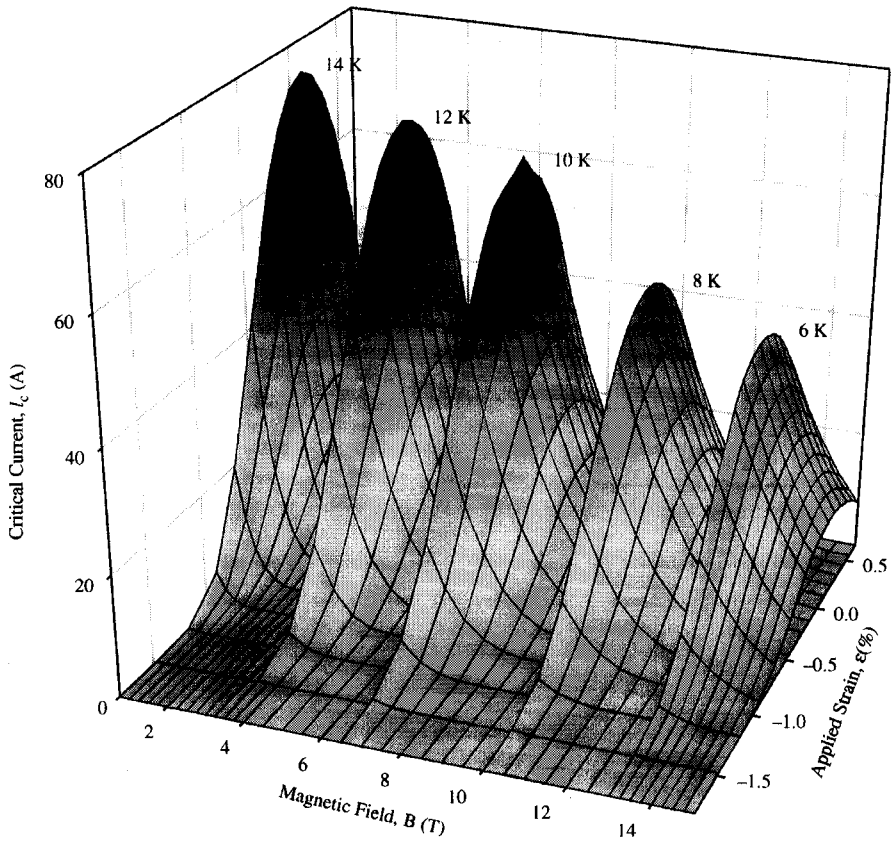

Figure C2.3.7. The four-dimensional critical-current surface of a Nb_3Al strand as a function of magnetic field, temperature and strain [76].

demonstrated that the effect of transverse stress is critically dependent on how the stress is applied. If the stress is localized, the effect on J_C is far more marked than if the stress is uniformly applied. This can be seen by comparing the degradation of J_C between round and flat conductors [77, 79].

Critical-current measurements have also been performed as a function of stress to estimate the strength of a conductor. In this case, the sample was loaded to a certain stress level and then unloaded to zero stress at room temperature. The conductor was then cooled to 4.2 K and the critical-current was measured. The variation of critical-current as a function of repeated applied stress at room temperature has been measured and the strength distribution for the composite calculated [80].

C2.3.5 Concluding remarks

The development of reliable techniques for testing conductors is essential to underpin a mature technology based on superconductivity and a better understanding of the underlying science. In light of the new complex composite conductors that are continuously being developed, the international community is committed to improving the testing of conductors. Domestic and international

programmes for laboratory intercomparisons of mechanical, thermal and electromagnetic measurements are in progress. This review has provided an introduction to testing the current carrying capacity of conductors. We hope that it contributes to improving the progress of scientists new to such work, towards better measurements techniques.

Acknowledgments

One of the authors (SAK) wishes to thank the UK Engineering and Physical Sciences Research Council (EPSRC) and Oxford Instruments P.L.C for their support. The authors thank Prof. K. Osamura and Dr L. Goodrich for their help in providing literature for this paper and P.A. Russell and S.J. Dunn for their help with producing the figures and the text.

References

[1] Tachikawa K 1995 Critical current measurement method for Nb_3Sn multifilamentary composite conductors foreward *Cryogenics* **35** S5
[2] Gould D and Wada H 1995 Introduction *Cryogenics* **35** S7
[3] Osamura K, Sato K and Furuto Y 1997 Standardization of the test methods for industrial superconductors by IEC/TC90 *Cryogenic Eng.* **32** 663
[4] Osamura K 1998 Present status of international standardization *ISTEC Journal* **11** 26
[5] Wilson M 1998 *Superconducting Magnets* (Oxford: Oxford University Press)
[6] Goodrich L F and Fickett F R 1982 Critical current measurements: a compendium of experimental results *Cryogenics* **22** 225
[7] Grasso G and Flükiger R 1997 Development of rectangular Bi(2223) wires with reduced anisotropy *Supercond. Sci. Technol.* **10** 223
[8] Goodrich L F and Bray S L 1989 Integrity tests for high-T_C and conventional critical-current measurement systems *Adv. Cryo. Eng. (Mater.)* **36A** 43
[9] Herrmann P F 1998 Current leads *Handbook of Applied Superconductivity*, ed B Seeber (Bristol: Institute of Physics) p 801
[10] White G K 1987 *Experimental Techniques in Low-Temperature Physics* 3rd edn (Oxford: Oxford University Press)
[11] White G K 1998 Thermal expansion *Handbook of Applied Superconductivity*, ed B Seeber (Bristol: Institute of Physics Publishing) p 1107
[12] Meingast C, Kraut O, Wolf T, Wühl H, Erb A and Müller-Vogt G 1991 Large $a-b$ anisotropy of the expansivity anomaly at T_C in untwinned $YBa_2Cu_3O_{7-d}$ *Phys. Rev. Lett.* **67** 1634
[13] Clark A F, Fujii G and Ranney M A 1981 The thermal expansion of several materials for superconducting magnets *IEEE Trans. Mag.* **17** 2316
[14] Okaji M, Nara K, Kato H, Michishita K and Kubo Y 1994 Thermal expansion of some advanced ceramics applicable as specimen holders of high T_c superconductors *Cryogenics* **34** 163
[15] Yamada N, Nara K, Okaji M, Hikata T, Kaneko T and Sadakata N 1998 Effect of thermal cycles on thermal expansion of silver-sheathed Bi2223 tape at 10–310 K *Cryogenics* **38** 397
[16] Kirchmayr H, Siddall M B and Smathers D B 1995 Effects of mandrel materials *Cryogenics* **35** S93
[17] Goodrich L F and Srivastava A N 1995 Thermal contraction of materials used in Nb_3Sn critical-current measurements *Cryogenics* **35** S29
[18] Clark A F 1983 Thermal expansion *Materials at Low Temperatures*, ed R P Reed and A F Clark (Ohio: American Society of Metals) p 75
[19] Pobell F 1992 *Matter and Methods at Low Temperatures* (Berlin: Springer)
[20] Cheggour N and Hampshire D P 2000 A probe for investigating the effect of magnetic field, temperature and strain on transport critical currents in superconducting tapes and wires *Rev. Sci. Instrum.* **71** 4521
[21] Ekin J W 1978 Current transfer in multifilamentary superconductors: I Theory *J. Appl. Phys.* **49** 3406
[22] Polak M, Zhang W, Parrell J, Cai X Y, Polyanskii A, Hellstrom E E, Larbalestier D C and Majoros M 1997 Current transfer lengths and the origin of linear components in the voltage–current curves of Ag-sheathed BSCCO components *Supercond. Sci. Technol.* **10** 769
[23] Ekin J W 1989 Offset criterion for determining superconductor critical current *Appl. Phys. Lett.* **55** 905
[24] Goodrich L F, Ekin J W and Fickett F R 1982 Effect of twist pitch on short-sample $V-I$ characteristics of multifilamentary wires *Adv. Cryo. Eng. (Mater.)* **28** 571
[25] Goodrich L F and Srivastava A N 1990 Software techniques to improve data reliability in superconductor and low-resistance measurements *J. Res. Natl Inst. Stand. Technol.* **95** 575

[26] Goodrich L F 1991 High T_C superconductor voltage–current simulator and the pulse method of measuring critical current *Cryogenics* **31** 720
[27] Goodrich L F, Wiejaczka J A, Srivastava A N, Stauffer T C and Medina L T 1995 USA interlaboratory comparison of superconductor simulator critical current measurements *IEEE Trans. Appl. Supercond.* **5** 548
[28] VAMAS Technical Working Party for Superconducting Materials 1995 Recommended standard method for determination of d.c. critical current of Nb_3Sn multifilamentary composite superconductor *Cryogenics* **35** S105
[29] Clark R G and Jones H 1986 The combination of dilution refrigerators and superconducting/hybrid magnets on physics research *Proc. 11th International Cryogenic Engineering Conference* p 414
[30] Itoh K, Tanaka Y and Osamura K 1986 Round robin test for the method of critical current measurement of Nb_3Sn composite conductors *Proc. 16th International Cryogenic Engineering Conference* p 1787
[31] Baixeras J and Fournet G 1967 Pertes par deplacement de vortex dans un supraconductor de type II non ideal *J. Phys. Chem. Solids* **28** 1541
[32] Willén D W A, Zhu W and Cave J R 1997 Selection of the offset-criterion voltage parameter and its relation to the second differential of a superconductor's voltage–current curve *Inst. Phys. Conf. Ser.* **158** 1013
[33] Hampshire D P and Jones H 1985 Critical current of a NbTi reference material as a function of field and temperature *Proc. Magnet Technol.* **9** 531
[34] Cai X Y, Polyanskii A, Li Q, Riley G N Jr and Larbalestier D C 1998 Current-limiting mechanisms in individual filaments extracted from superconducting tapes *Nature* **392** 906
[35] Hampshire D P and Jones H 1987 Analysis of the general structure of the E–I characteristic of high current superconductors with particular reference to a Nb–Ti SRM wire *Cryogenics* **27** 608
[36] Hampshire D P and Jones H 1987 A detailed investigation of the E–J characteristic and the role of defect motion within the flux-line lattice for high-current-density, high-field superconducting compounds with particular reference to data on Nb_3Sn throughout its entire field-temperature phase space *J. Phys. C: Solid State Phys.* **20** 3533
[37] Hampshire D P, Clark A F and Jones H 1989 Flux pinning and scaling laws for superconducting V_3Ga *J. Appl. Phys.* **66** 3160
[38] Edelman H S and Larbalestier D C 1993 Resistive transitions and the origin of the n value in superconductors with a Gaussian critical current distribution *J. Appl. Phys.* **74** 3312
[39] Ryan, D T Critical-currents of commercial superconductors in the picovolt per metre electric field regime *PhD Thesis* University of Oxford
[40] Warnes W H and Larbalestier D C 1986 Critical current distributions in superconducting composites *Cryogenics* **26** 643
[41] Goodrich L F, Srivastava A N, Yuyama M and Wada H 1993 n-value and second derivative of the superconductor voltage–current characteristic *IEEE Trans. Appl. Supercond.* **3** 1265
[42] Yamafuji K and Kiss T 1997 Current–voltage characteristics near the glass–liquid transition in high-T_c superconductors *Physica* C **290** 9
[43] Cheggour N and Hampshire D P 1997 The role of vortex melting and inhomogenieties in the transport properties of Nb_3Sn superconducting wires *Inst. Phys. Conf. Ser.* **158** 1275
[44] Lide D R 1992 *CRC Handbook of Chemistry and Physics* (Boca Raton: CRC Press)
[45] Goodrich L F, Bray S L and Stauffer T C 1990 Thermal contraction of fibreglass-epoxy sample holders used for Nb_3Sn critical-current measurements *Adv. Cryo. Eng. (Mater.)* **36** 117
[46] Wiejaczka J A and Goodrich L F 1997 Interlaboratory comparison on high-temperature superconductor critical-current measurements *J. Res. Natl. Inst. Stand. Technol.* **102** 29
[47] Marti F, Grasso G, Huang Y and Flükiger R 1997 High critical current densities in long lengths of mono- and multifilamentary Ag-sheathed Bi(2223) tapes *IEEE Trans. Appl. Supercond.* **7** 2215
[48] Goodrich L F Critical-current measurement methods for oxide superconductor tapes and wires. Part 1: transport current method *Cryogenics Submitted*
[49] Küpfer H and Gey W 1977 Dependence of the critical current density of superconductors on the past history of the magnetic field and the temperature *Phil. Mag.* **36** 859
[50] Goodrich L F, Vecchia D F, Pittman E S, Ekin J W and Clark A F 1984 Critical-current measurements on an NbTi superconducting wire standard reference material *NBS Spec. Publi.* 1
[51] Goodrich L F and Srivastava A N 1995 Critical current measurement methods: quantitative evaluation *Cryogenics* **35** S19
[52] Ogawa R, Kubo Y, Tanaka Y, Itoh K, Ohmatsu K, Kumano T, Sakai, S and Osamura K 1996 Standardization of the test method for critical current measurement of Cu/Cu–Ni/Nb–Ti composite superconductors *Proc. 16th International Cryogenic Engineering Conference* p 1799
[53] VAMAS Technical Working Party for Superconducting Materials, 1995 Second intercomparison of critical current measurements *Cryogenics* **35** S65
[54] Kirchmayr H 1995 Effects of specimen bonding materials *Cryogenics* **35** S95
[55] Sneary A B, Friend C M, Vallier J C and Hampshire D P 1999 Critical current density of Bi-2223/Ag multifilamentary tapes from 4.2 K up to 90 K in magnetic fields up to 23 T *IEEE Trans. Appl. Supercond.* **9** 2585
[56] International Electrotechnical Commission (1999) Critical current measurement dc critical current of Ag-sheathed Bi-2212 and Bi-2223 oxide superconductors IEC61788-3

[57] Goodrich L F and Srivastava A N 1992 Comparison of transport critical current measurement methods *Adv. Cryo. Eng. (Mater.)* **38** 559
[58] Hole. C R J Pulsed magnetic field characterisation of technological high temperature superconductors *PhD Thesis* University of Oxford
[59] Ryan D T, Jones H, Timms W and Killoran N 1997 Critical current measurements at electric fields in the pV m^{-1} regime *IEEE Trans. Appl. Supercond.* **7** 1455
[60] Friend C M and Hampshire D P 1995 A probe for the measurement of the transport critical-current density of superconductors in high magnetic fields and at temperatures between 2 and 150 K *Meas. Sci. Technol.* **6** 98
[61] Frost A J, Jones H and Belenli I 1992 Design, construction and development of an apparatus for the transport-current characterization of high-temperature superconductors at a range of temperatures and magnetic fields *Cryogenics* **32** 1014
[62] Kuroda T, Murakami Y, Itoh K, Yuyama M, Wada H and Mao D 1998 Temperature dependence of critical current density of Nb_3Al multifilamentary wires fabricated by Nb-tube and its improved processes *Cryogenics* **38** 785
[63] Goodrich L F, Medina L T and Stauffer T C 1997 High critical-current measurements in liquid and gaseous helium *Adv. Cryo. Eng. (Mater.)* **44** 873
[64] Ekin J W 1980 Strain scaling law for flux pinning in practical superconductors. Part 1: basic relationship and application to Nb_3Sn conductors *Cryogenics* **20** 611
[65] Kamata K, *et al* 1992 Superconducting properties and strain effects in high fields for bronze processed multifilamentary $(Nb,Ti)_3Sn$ wires and composite processed ultrafine Nb_3Al wires *Sci. Rep. Res. Inst. Tohoku Univ. Ser.* A – *Phys. Chem. Metall.* A **37** 99
[66] Fukutsuka T, Horiuchi T, Monju Y, Tatara I, Maeda Y and Moritoki M 1984 Effects of hot isostatic pressing on the superconducting properties of Nb_3Sn multifilamentary wires *Adv. Cryo. Eng.* **30** 891
[67] Takeuchi T, Iijima Y, Inoue K, Wada H, ten Haken B, ten Kate H H J, Fukuda K, Iwaki G, Sakai S and Moriai H 1997 Strain effects in Nb_3Al multifilamentary conductors prepared by phase transformation from bcc supersaturated-solid solution *Appl. Phys. Lett.* **71** 122
[68] Goldacker W, Specking W, Weiss F, Rimikis G and Flükiger R 1989 Influence of transverse compressive and axial tensile stress on the superconductivity of $PbMo_6S_8$ and $SnMo_6S_8$ wires *Cryogenics* **29** 955
[69] Ekin J W, Finnemore D K, Li Q, Tenbrink J and Carter W 1992 Effect of axial strain on the critical-current of Ag-sheathed Bi-based superconductors in magnetic fields up to 25 T *Appl. Phys. Lett.* **61** 858
[70] Goldacker W, Keßler J, Ullmann B, Mossang E and Rikel M 1995 Axial tensile, transverse compressive and bending strain experiments in Bi(2223)/AgMg single core tapes *IEEE Trans. Appl. Supercond.* **5** 1834
[71] Richens P E, Jones H, van Cleemput M and Hampshire D P 1997 Strain dependence of critical-currents in commercial high temperature superconductors *IEEE Trans. Appl. Supercond.* **7** 1315
[72] Ten Haken, B Strain effects on the critical properties of high-field superconductors *PhD Thesis* Technical University of Twente
[73] Walters C R, Davidson I M and Tuck G E 1986 Long sample high sensitivity critical-current measurements under strain *Cryogenics* **26** 406
[74] ten Haken B, Godeke A and ten Kate H H J 1999 The strain dependence of the critical properties of Nb_3Sn conductors *J. Appl. Phys.* **85** 3247
[75] Cheggour N and Hampshire D P 1999 Unifying the strain and temperature scaling laws for the pinning force density in superconducting niobium–tin multifilamentary wires *J. Appl. Phys.* **86** 552
[76] Keys S A, Koizumi N, Hampshire D P, Strain scaling in Nb_3Al unpublished
[77] Ekin J W 1987 Effect of transverse compressive stress on the critical current and upper critical field of Nb_3Sn *J. Appl. Phys.* **62** 4829
[78] ten Kate H H J, Weijers H W and van Oort J M 1993 Critical current degradation in Nb_3Sn cables under transverse pressure *IEEE Trans. Appl. Supercond.* **3** 1334
[79] Jakob B, Pasztor G, Bona M and Asner A 1991 Reduced sensitivity of Nb_3Sn epoxy-impregnated cable to transverse stress *Cryogenics* **31** 390
[80] Ochiai O, Osamura K and Watanabe K 1993 Estimation of strength distribution of Nb 3Sn in multifilamentary composite wire from change in superconducting current due to preloading *J. Appl. Phys.* **74** 440

Author Queries

JOB NUMBER: C2.3
JOURNAL: HSM

Q1 Affiliation and Abstract missing in the text. Please check.